Radiation Protection Dosimetry Advance Access published April 21, 2016

Radiation Protection Dosimetry (2016), pp. 1–15 doi:10.1093/rpd/ncw096

ASSESSMENT OF THE ABSORBED DOSE IN THE KIDNEY OF NUCLEAR NEPHROLOGY PAEDIATRIC PATIENTS USING ICRP BIOKINETIC DATA AND MONTE CARLO SIMULATIONS WITH MASS-SCALED PAEDIATRIC VOXEL PHANTOMS

P. Teles[1,*], M. Mendes[1], M. Zankl[2], V. de Sousa[1], A. I. Santos[3] and P. Vaz[1]
[1]Grupo de Protecção e Segurança Radiológica, Centro de Ciências e Tecnologias Nucleares (C2TN), CTN/IST, Pólo de Loures. Estrada Nacional 10 (km 139,7), 2695-066 Bobadela LRS, Portugal
[2]Helmholtz Zentrum München – German Research Center for Environmental Health (HMGU), Department of Radiation Sciences, Research Unit Medical Radiation Physics and Diagnostics, Ingolstaedter Landstr. 1, 85764 Neuherberg, Germany
[3]Serviço de Medicina Nuclear, Hospital Garcia de Orta, E.P.E. Av. Torrado da Silva, 2801-951 Almada, Portugal

*Corresponding author: ppteles@ctn.ist.utl.pt

The aim of this work is to use Monte Carlo simulations and VOXEL phantoms to estimate the absorbed dose in paediatric patients (aged from 2 weeks to 16 y), with normal renal function, to whom technetium-99m-dimercaptosuccinic acid (^{99m}Tc-DMSA) was administered, for diagnostic renal scintigraphy purposes; and compare them with values obtained using the International Commission on Radiological Protection (ICRP) methodology. In the ICRP methodology, the cumulated absorbed dose in the kidneys is estimated by multiplying the administered activity with the corresponding given dose coefficients. The other methods were based on Monte Carlo simulations performed on two paediatric voxel phantoms (*CHILD* and *BABY*), and another three phantoms, which were modified to suit the mass of the patients' kidneys, and other anatomical factors. Different *S*-values were estimated using this methodology, which together with solving the ICRP biokinetic model to determine the cumulated activities, allowed for the estimation of absorbed doses different from those obtained with the ICRP method, together with new dose coefficients. The obtained values were then compared. The deviations suggest that the *S*-values are strongly dependent on the patient's total body weight, which could be in contrast with the ICRP data, which is provided by age, regardless of other anatomical parameters.

INTRODUCTION

The growing use of ionising radiation in medicine has improved overall diagnosis and prognosis for many diseases. However, the population dose due to medical exposures has also increased significantly[1], including in nuclear medicine procedures. This is particularly worrisome for paediatric patients[2]. In the USA, the total number of nuclear medicine procedures has increased almost 3-fold from 6.3 to 18.1 million procedures from 1984 to 2006, with approximately 1% of these being performed on children[3, 4]. According to a new UNSCEAR Committee report[5], babies, children and adolescents are at a considerably higher risk of radiation-induced cancer than adults. The Committee reviewed 23 different types of cancer, and for about 25% of them (including leukaemia, thyroid, skin, breast and brain cancer) children were clearly more radiosensitive. In the case of solid tumours, for a fixed radiation dose, a 10-year-old person is at about twice the risk, and a newborn at about three times the risk, than a 40-year-old person[6]. In the more specific case of nuclear medicine, given the significant amount of examinations, and despite the fact that administered activities are low, it is necessary to properly quantify the potential risks associated with the use of radiopharmaceuticals, from a radiological protection viewpoint. In fact, a correct dosimetric assessment of radiopharmaceutical intake associated with a nuclear medicine procedure can significantly lead to the optimisation of the absorbed dose, improvement of the guidelines, and therefore, lead to minimising risk. Although there is no straightforward way to determine the 'actual' absorbed dose inside the human body, the formalism of the Medical Internal Radiation Dose (MIRD) Committee of the Society of Nuclear Medicine has been adopted as the International Commission on Radiological Protection (ICRP) calculation method for estimating radiation doses to organs from radionuclides distributed inside the body[7]. In the MIRD formalism, the time-integrated activity in each source region and the mean absorbed dose to the target organ per unit of nuclear transition are used to determine the absorbed dose to a target organ. The time-integrated activity may be obtained by solving biokinetic models. Biokinetic data for a large number of radionuclides were published by the ICRP in ICRP Publication 53[8],

© The Author 2016. Published by Oxford University Press. All rights reserved. For Permissions, please email: journals.permissions@oup.com

Downloaded from http://rpd.oxfordjournals.org/ at City University, London on April 23, 2016

and updated in the ICRP Publication 128[9]. MIRD pamphlet 21 deals with the nomenclature standardisation between ICRP and MIRD[10]. However, despite this, and given the continuous advances in nuclear medicine, the biokinetic data, for many nuclear medicine procedures, more specifically in the case of children, can be and have been challenged. In fact, most of the research in this topic indicates that uncertainties are deemed very high[11].

Leggett *et al.*[12] argue that the uncertainties associated with biokinetic models are the largest sources of error in calculating the dose per unit of incorporated activity in nuclear medicine, not quantifying them. Further uncertainties are introduced by the anatomical differences between patients and the stylised models of the human body used for the determination of ICRP's internal organ dose coefficients up to now. Zankl *et al.*[13] report that, when comparing calculations using voxel phantoms with calculations using stylised ('MIRD-type') phantoms, deviations between 50 and 100% can be obtained. And finally, Hadid *et al.*[14, 15] and Parach *et al.*[16] reach similar conclusions, showing that when calculating dose coefficients with voxel phantoms and comparing them with a MIRD phantom, significant variations (up to few hundred percent) were obtained.

Therefore, there is a considerable interest in investigating the radiation dose and its effects[17, 18], in paediatric nuclear medicine patients. New dosimetric data in paediatric patients can be obtained with state-of-the-art techniques. Gathering a great collection of such data can then potentiate a better understanding of the biokinetics of different radiopharmaceuticals, and eventually lead to the optimisation of clinical protocols, and perhaps even contribute to reducing the dose to which paediatric patients are exposed, without affecting diagnostic outcomes.

This work aims at contributing to improve and complement such studies. The absorbed dose in 17 paediatric patients of different ages administered with technetium-99m-dimercaptosuccinic acid (^{99m}Tc-DMSA), used in routine paediatric nuclear medicine for kidney disorder diagnostics, is estimated by means of biokinetic models and MC simulations using voxel phantoms. The obtained *S*-values were compared with values obtained from the available ICRP models and deviations were determined. Dose coefficients were also determined and compared with those available in the literature.

MATERIALS AND METHODS

Patient data

Seventeen paediatric patients with normal renal function were injected with a radiopharmaceutical containing ^{99m}Tc-DMSA at the Hospital Garcia de Orta (HGO) in Almada, Portugal. Information about the patients can be found in Table 1.

Biokinetic model

The activity curves as functions of time in the kidneys and other organs of interest were built using the available ^{99m}Tc-DMSA biokinetic data from ICRP Publications 53[8] and 128[9] (*The biokinetic data from ICRP Publications 53 and 128 will be referred as ICRP model from now on. The models in*

Table 1. Description of the 17 paediatric patients administered with ^{99m}Tc-DMSA.

Patient	Sex	Age	Weight (kg)	Administered activity (MBq)
1	M	2 months	3.4	25.16
2	M	8 months	10.0	38.85
3	M	10 months	9.0	37.00
4	M	10 months	11.0	37.00
5	M	12 months	13.0	48.10
6	M	13 months	10.0	39.96
7	F	16 months	10.0	42.92
8	F	17 months	11.0	41.81
9	F	2 y	13.5	41.81
10	F	2 y	12.0	38.48
11	F	3 y	17.6	58.09
12	M	4 y	15.0	44.40
13	F	11 y	40.0	70.30
14	F	11 y	43.5	77.33
15	M	15 y	50.0	85.10
16	M	15 y	78.0	129.50
17	F	16 y	62.0	92.50

Downloaded from http://rpd.oxfordjournals.org/ at City University, London on April 23, 2016

Publications 53 and 128 are identical) and ICRP Publication 106[19].

Assuming immediate uptake of the administered activity A_0, the activity as a function of time $A_S(t)$, in the source organ S, with an effective half-life $T_{i,\text{eff}}$, can be expressed as

$$\frac{A_S(t)}{A_0} = F_S \sum_{i=1}^{n} a_i e^{\left(\frac{-\ln 2}{T_{i,\text{eff}}} t\right)}, \quad (1)$$

where F_S is the fraction of the administered radiopharmaceutical incorporated by the organ S; a_i is the fraction of F_S eliminated with a biological half-life T_i; and n is the number of elimination components. The effective half-life, $T_{i,\text{eff}}$, is given by Equation 2, where T_i and T_p are the biological and physical half-life, respectively[18].

$$\frac{1}{T_{i,\text{eff}}} = \frac{1}{T_i} + \frac{1}{T_p} \quad (2)$$

The cumulated activity, $\tilde{A}_S$, is given by Equation 3, which is the quantity that is used to determine the absorbed dose, by making use of the ICRP dose coefficients.

$$\frac{\tilde{A}_S}{A_0} = F_S \sum_{i=1}^{n} a_i \frac{T_{i,\text{eff}}}{\ln 2} \quad (3)$$

The ICRP biokinetic model states that, after ^{99m}Tc-DMSA is intravenously injected on a subject, it is distributed in the extracellular fluid. Once inside the extracellular fluid, half is deposited in the renal cortex (hence $F_s = 0.5$ in the kidneys), where it is retained for a long period of time. Also, and as shown in Table 2, a further fraction is temporarily retained in the liver and spleen. Hereupon, when referring to the ICRP model, a fraction of 0.5 is taken up in the renal cortex, with an uptake half-time of 1 h, and it is assumed to be retained permanently. Fractions of 0.1 and 0.01 are taken up in the liver and spleen with a half-time of 1 h and cleared with half-times of 2 h (0.5) and 1.8 d (0.5). This radiopharmaceutical is excreted exclusively via the kidneys, which makes them an important source region for the radiation dosimetry of this substance. The biokinetic model is constructed for adults, and it is possible that physiological and biokinetic values are different in children and adolescents, however this is beyond the scope of this work, which intends to look at dosimetric data. Finally, it should be noted that, in this study, no blood data was taken.

Monte Carlo simulations

Software and paediatric voxel phantoms

The simulations were performed using the state-of-art MCNPX 2.7.0 computer program developed by the Los Alamos National Laboratory (LANL)[20] and two paediatric voxel phantoms *BABY* (8 weeks) and *CHILD* (7 y) that are shown in Figure 1. These phantoms were developed at the Helmholtz

Table 2. Biokinetic data of ^{99m}Tc-DMSA from ICRP Publications 53 and 128 for the organs of interest in body biodistribution of the radiopharmaceutical[8].

Organ	F_s	T_i (h)	a_i	$\tilde{A}_s/A_0$ (h)
Total body[a]	1.0	2.0	0.25	6.8
		43	0.25	
		∞	0.5	
Kidneys	0.5	1.0	−1	3.7
		∞	1	
Liver	0.1	1.0	−1	0.42
		2.0	0.5	
		43	0.5	
Spleen	0.01	1.0	−1	0.042
		2.0	0.5	
		43	0.5	
Urinary bladder contents	0.50			0.40

[a]It excludes urinary bladder content. 'Total Body' is called 'other' in this work.

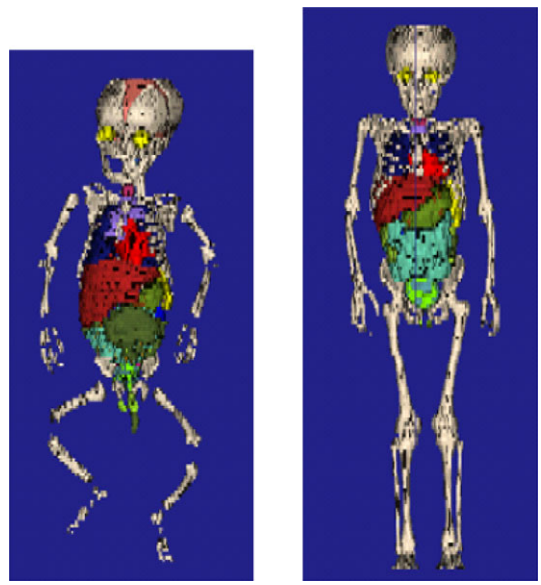

Figure 1. Paediatric voxel phantoms *BABY* (left) and *CHILD* (right).

Downloaded from http://rpd.oxfordjournals.org/ at City University, London on April 23, 2016

Table 3. Main features of the voxel phantoms *BABY* and *CHILD*.

	BABY	CHILD
Gender	F	F
Age	8 weeks	7 y
Height (cm)	57	115
Weight (kg)	4.2	21.7
Kidney mass (g)	30.3	188.8
Matrix dimension	267 × 138 × 142	256 × 256 × 144
Original dimensions of the voxels	(0.085 × 0.085 × 0.4 = 0.00289) cm^3	(0.154 × 0.154 × 0.8 = 0.01897) cm^3

Zentrum München—German Research Center for Environmental Health (HMGU)[21]. Table 3 reports the main features of these two phantoms.

Considering the large variability of the patients (weight and age), in order to obtain more accurate results, the voxel dimensions of the phantoms (*BABY* and *CHILD*) were modified to fit the anatomy of the patients more accurately. Therefore, besides the aforementioned *BABY* and *CHILD* phantoms, another four voxel phantoms (*Baby_9.5 kg*, *Child_13.2 kg*, *Child_21.5 kg* and *Child_30 kg*) were created by scaling the voxels of the two original phantoms. The ICRP anatomical information to create these new voxel phantoms, that is, the body height and kidney mass for 1-, 5-, 10- and 15-year-old children, was taken from ICRP Publication 89[20].

The parameters by which the new voxel phantoms were scaled were:

(a) The ICRP kidney mass from ICRP 89, by knowing the number of voxels that correspond to the two kidneys, and knowing that the kidney density does not change, a new volume can be determined for a different mass by simple proportionality.
(b) The body height values. The *z* dimension of the voxels was scaled so the condition for the new volume determined in item (a) could be satisfied.

Subsequently, the *x*- and *y*-dimensions were scaled accordingly, preserving the proportionality of item (a). The rest of the anatomical data can then be estimated from this. Although this is a practical method to match the kidney mass and the height to the ICRP value, there are still significant deviations in the masses of the other organs and the scaling of the phantoms introduces another source of uncertainty, as the distances between organs' centres of mass will also vary, and this can have influence in the cross-fire *S*-values. For instance the chord length (defined as the distance between the organs' centres of mass) between the liver and the right kidney varies in the CHILD phantom, as it is scaled, from 5.84 cm to 7.68 cm. However, since, in the case of this study, the main influence in the absorbed dose will be the self-absorption *S*-value, the geometric variations will have a minor impact, and it is beyond the scope of this work to determine their influence.

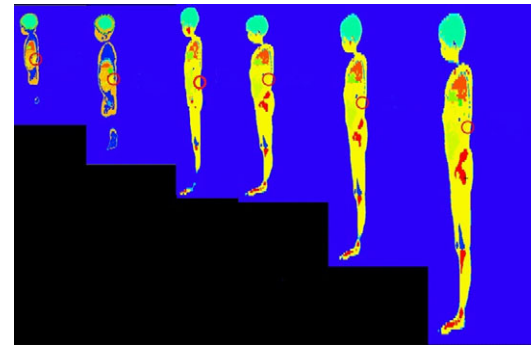

Figure 2. Implemented voxel phantoms *Baby_4.2 kg (original Baby phantom)* (left), *Baby_9.5 kg*, *Child_13.2 kg*, *Child_21.7 kg (original child phantom)*, *Child_21.5 kg* and *Child_30 kg* (right), all at the same YZ cut. The kidneys (region where energy deposition was calculated) are marked with a red circle.

Although the weight of patient 1 is closer to that of a newborn, the ICRP dose conversion coefficient for the 1 year old had to be used, since ICRP does not provide dose coefficients for newborns.

The new voxel phantoms were named according to their weight:

- *Baby_4.2 kg*, the original BABY phantom, with 51 cm height and 30 g kidney mass,
- *Baby_9.5 kg* with 76 cm height and 70 g kidney mass, the same values as for ICRP 89 1 year old,
- *Child_13.2 kg* with 109 cm height and 104.8 kidney mass, the same values as for the ICRP 89 5 years old,
- *Child_21.5 kg* with 138 cm height and 180 g kidney mass, the same values as for the ICRP 89 10 years old,
- *Child_21.7 kg*, the original CHILD phantom, with 115 cm height and 188.8 g kidney mass,

Downloaded from http://rpd.oxfordjournals.org/ at City University, London on April 23, 2016

Table 4. Comparison between organ masses and height from ICRP Publication 89 and the four voxel phantoms used in this study.

This paper's nomenclature	ICRP 89 correspondence		Organ mass (g)				Dimensions (cm)			
			Kidneys (2)	Liver	Spleen	Body weight (kg)	*x*	*y*	*z*	*z* (ICRP height)
Baby_4.2 kg	Newborn	ICRP	25	130	9.5	3.5	22.70	11.73	56.8	51
		Voxel phantom	30.3	182	15	4.2				
		Dev (%)	21.2	40	57.9	16.6				
		Ratio	0.8	0.7	0.6					
Baby_9.5 kg	1 year old	ICRP	70	330	29	10	29.90	15.45	76	76
		Voxel phantom	70	421	34	9.5				
		Dev (%)	0.0	27.5	16.7	−5.2				
		Ratio	1.0	0.8	0.9					
Child_13.2 kg	5 years old	ICRP	110	570	50	19	30.98	30.98	109	109
		Voxel phantom	110	429	89	13.2				
		Dev (%)	0.0	−31.7	60.6	−43.9				
		ratio	1.0	1.3	0.6					
Child_21.5 kg	10 years old	ICRP	180	830	80	32	35.07	35.07	138	138
		Voxel phantom	180	702	145	21.5				
		Dev (%)	0.0	−15.4	81.1	−48.8				
		ratio	1.0	1.2	0.6					
Child_21.7 kg	10 years old	ICRP	180	830	80	32	39.42	39.42	115	138
		Voxel phantom	188	733	151	21.7				
		Dev (%)	4.4	−11.7	88.8	−47.4				
		ratio	1.0	1.1	0.5					
Child_30 kg	15 years old	ICRP	250	1300	130	56	37.63	37.63	167	167
		Voxel phantom	250	975	201	30				
		Dev (%)	0.0	−25.0	54.7	−86.7				
		ratio	1.0	1.3	0.6					

Downloaded from http://rpd.oxfordjournals.org/ at City University, London on April 23, 2016

- *Child_30 kg*, with 167 cm height and 250 g kidney mass, respectively, the same values as for the ICRP 89 15-year male child, because the patients aged 15 or more in this study were mostly male.

A depiction of the VOXEL phantoms obtained with this method is shown in Figure 2. Table 4 shows the organ masses for the ICRP kidneys, liver and spleen, total height, from ICRP 89 and from the voxel phantoms and the respective deviations (%), and ratios, between them.

As can be seen in Table 4, there are significant variations between the liver and spleen mass for the five phantoms relative to the ICRP 89 values.

For *Baby_9.5 kg*, the liver and spleen are larger than the ICRP values. For *Child_21.5 kg* and *Child_30 kg* the spleen is significantly larger than ICRP, while the liver is smaller. It is also important to notice that the full body weight of the voxel phantoms is always smaller than the ICRP values, decreasing with age, leading to almost half the weight value than the body weights of the patients within the age range of 15 y. In this case, the adult GSF voxel phantom[15] could have been scaled to match the kidney mass and the height of the 15-year-old child, but this would be beyond the scope of this work (which is to use child voxel phantoms to estimate absorbed dose). Also, it would have led to values with no significant variation to absorbed dose determined with ICRP since that is, overall, the ICRP methodology (scaling adult voxel phantoms to fit the anatomical parameters of children of different ages). In fact, in the age-specific MIRD-type phantoms (Cristy and Eckerman[22]), considerations on human anatomical growth with age have been taken into account, but these differences will be very small for the 15-year-old child. It should be noted, however, that in this study a voxel phantom of a 7-year-old child is used to determine the *S*-values for 15-year-old children.

In order to determine the dose and other parameters, each patient was ascribed with one of the voxel phantoms, which was its closest ICRP match (defined as age) or by total weight[23].

In cases where the closest matches by weight, and by age, were different, both phantoms were used for absorbed dose calculations, and the resulting values were compared with ICRP values, as shown in Table 5.

S-value estimations using MC simulations

^{99m}Tc sources were simulated separately in the kidneys, liver, spleen and total body of the paediatric voxel phantoms. Photons and betas were considered as emitted particles[24]. In order to have low statistical errors ($1\sigma < 3\%$), 10^9 particles were simulated. Tally F6 (deposited energy per mass in a cell per emitted particle of the source in MeV/g) was used to obtain the absorbed dose in the kidneys. One can clearly see that this is, in fact, in the MIRD formalism, the same as determining the *S*-value. Multiplying this *S*-value for each phantom ascribed to a patient by the cumulated activity values, the absorbed dose in the kidneys can be determined, using the phantom closest to the patient both by total body weight or by age (method 1 or method 2).

The kidney mass and the distances between the kidneys and the various source organs, that is, the anatomy of the phantom, will have an impact in the energy deposited in the kidneys MC simulations. In fact, the distance between source and target region is a parameter that influences the specific absorbed fractions in internal dosimetry[25], which is not taken into account in this study.

Table 5. Description of the 17 paediatric patients administered with ^{99m}Tc-DMSA.

Patient	Sex	Age	Weight (kg)	Closest match to ICRP	Closest match by weight
1	M	2 months	3.4	Baby_9.5 kg	Baby_4.3 kg
2	M	8 months	10.0	Baby_9.5 kg	Baby_9.5 kg
3	M	10 months	9.0	Baby_9.5 kg	Baby_9.5 kg
4	M	10 months	11.0	Baby_9.5 kg	Child_13.2 kg
5	M	12 months	13.0	Baby_9.5 kg	Child_13.2 kg
6	M	13 months	10.0	Baby_9.5 kg	Baby_9.5 kg
7	F	16 months	10.0	Baby_9.5 kg	Baby_9.5 kg
8	F	17 months	11.0	Baby_9.5 kg	Child_13.2 kg
9	F	2 y	13.5	Baby_9.5 kg	Child_13.2 kg
10	F	2 y	12.0	Baby_9.5 kg	Child_13.2 kg
11	F	3 y	17.6	Child_13.2 kg	Child 21.5 kg
12	M	4 y	15.0	Child_21.5 kg	Child_13.2 kg
13	F	11 y	40.0	Child_21.5 kg	Child_30 kg
14	F	11 y	43.5	Child_21.5 kg	Child_30 kg
15	M	15 y	50.0	Child_30 kg	Child_30 kg
16	M	15 y	78.0	Child_30 kg	Child_30 kg
17	F	16 y	62.0	Child_30 kg	Child_30 kg

Downloaded from http://rpd.oxfordjournals.org/ at City University, London on April 23, 2016

RESULTS AND DISCUSSION

Biokinetic model activity curves

The ICRP model[8, 9] is used to build the activity curves as a function of time for each source region, following Equation 1. The administered activity A_0 is decided at the Nuclear Medicine Service of HGO, according to protocol and adopted guidelines[26]. Figure 3 shows the percentage activity per injected activity curves for all affected organs.

Also, for each patient the cumulated activity ($\tilde{A}$) is determined (estimated by the biokinetic model from ICRP 128 through Equation 3), which is shown in Table 6.

These values can be used to estimate the absorbed dose, by multiplying them with either the ICRP dose coefficients or, alternatively, the values estimated using MC simulations, using methods 1,2 or 3.

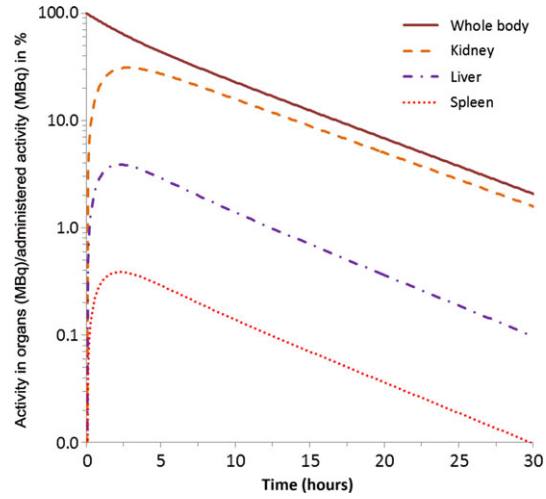

Figure 3. Percentage of activity in affected organs (MBq) per injected activity as a function of time (h) according to the biokinetic model from ICRP Publication 53, in log scale. Percentage activity in the kidney reaches a max of ~30% approximately 2 h after injection.

Monte Carlo results and absorbed dose estimation

Table 7 shows the Monte Carlo estimations of the *S*-values for the kidneys when a source of ^{99m}Tc is simulated in different organs, for the five used

Table 6. Cumulated activities in all important organs and regions, using the biokinetic model from ICRP Publication 53.

Patient	Kidneys (MBq)	Other (MBq)	Liver (MBq)	Spleen (MBq)	Bladder content (MBq)
1	3.37×10^5	6.15×10^5	3.31×10^4	3.31×10^3	3.62×10^4
2	5.21×10^5	9.50×10^5	5.11×10^4	5.11×10^3	5.59×10^4
3	4.96×10^5	9.04×10^5	4.87×10^4	4.87×10^3	5.33×10^4
4	4.96×10^5	9.04×10^5	4.87×10^4	4.87×10^3	5.33×10^4
5	6.45×10^5	1.18×10^6	6.33×10^4	6.33×10^3	6.93×10^4
6	5.36×10^5	9.77×10^5	5.26×10^4	5.26×10^3	5.75×10^4
7	5.75×10^5	1.05×10^6	5.65×10^4	5.65×10^3	6.18×10^4
8	5.61×10^5	1.02×10^5	5.50×10^4	5.50×10^3	6.02×10^4
9	5.61×10^5	1.02×10^6	5.50×10^4	5.50×10^3	6.02×10^4
10	5.16×10^5	9.41×10^5	5.07×10^4	5.07×10^3	5.54×10^4
11	7.79×10^5	1.42×10^6	7.65×10^4	7.65×10^3	8.36×10^4
12	5.95×10^5	1.09×10^6	5.85×10^4	5.85×10^3	6.39×10^4
13	9.42×10^5	1.72×10^6	9.26×10^4	9.26×10^3	1.01×10^5
14	1.04×10^6	1.89×10^6	1.02×10^5	1.02×10^4	1.11×10^5
15	1.14×10^6	2.08×10^6	1.12×10^5	1.12×10^4	1.23×10^5
16	1.74×10^6	3.17×10^6	1.70×10^5	1.70×10^4	1.86×10^5
17	1.24×10^6	2.26×10^6	1.22×10^5	1.22×10^4	1.33×10^5

Table 7. *S*-values in the kidneys for different source organs for the five voxel phantoms.

Source organ	Baby_4.2 kg	Baby_9.5 kg	Child_13.2 kg	Child_21.5 kg	Child_21.7 kg	Child_30 kg
	mGy/MBq					
Kidney	1.12×10^{-4}	5.20×10^{-5}	3.44×10^{-5}	2.20×10^{-5}	2.13×10^{-5}	1.64×10^{-5}
Liver	2.00×10^{-6}	1.16×10^{-6}	1.13×10^{-6}	7.80×10^{-7}	8.47×10^{-7}	5.96×10^{-7}
Spleen	3.36×10^{-6}	1.92×10^{-6}	1.52×10^{-6}	1.08×10^{-6}	1.08×10^{-6}	8.52×10^{-7}
Other	7.98×10^{-7}	4.47×10^{-7}	2.96×10^{-7}	2.00×10^{-7}	2.17×10^{-7}	1.50×10^{-7}
Bladder content	8.09×10^{-7}	4.47×10^{-7}	1.73×10^{-7}	1.45×10^{-7}	8.85×10^{-8}	4.90×10^{-8}

Downloaded from http://rpd.oxfordjournals.org/ at City University, London on April 23, 2016

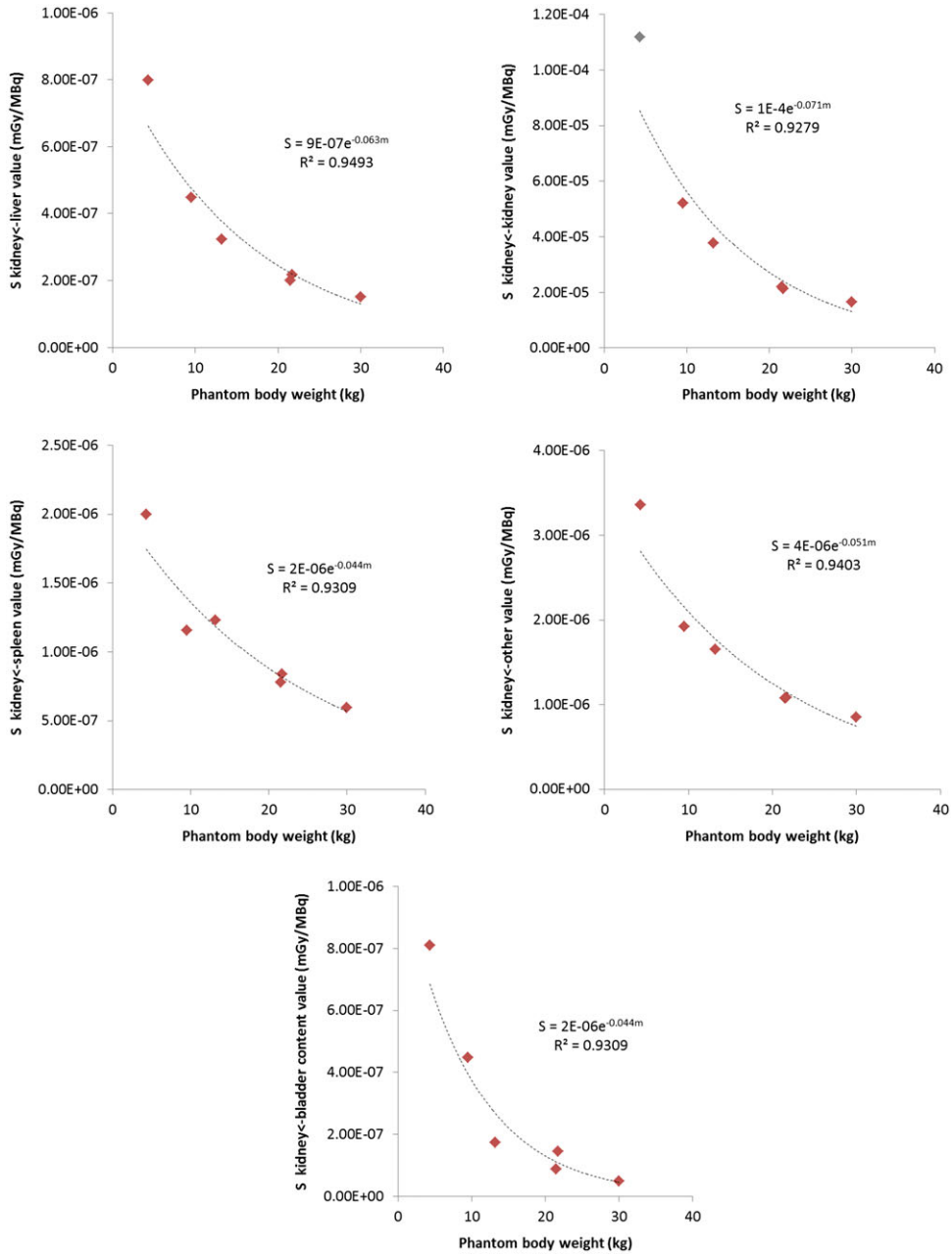

Figure 4. *S*-values as a function of the phantom body weight used to compute them. The lines represent the fit to an exponential function, the values of which are presented on top of the graphs.

phantoms. All values have less than 3% (1σ) statistical uncertainty.

The *S*-values for each organ of interest can be plotted as a function of the full body weight of the patient. The *S*-values seem to follow an exponential trendline. By fitting the MC *S*-value results with an exponential trendline, following the phenomenological Equation 4:

$$S = S_0 e^{-km}, \tag{4}$$

Downloaded from http://rpd.oxfordjournals.org/ at City University, London on April 23, 2016

where S_0 in units of mGy/MBq is the theoretical S-value where the total body mass $m \ll k$, and k is a 'mass constant' with units of kg^{-1}, the S-values for the real weight of the patient can be computed and used to determine the absorbed dose. This will be called method 3. The obtained functions are shown in Figure 4.

The S-values for each organ obtained in this way, take into account the real value of the patient's body, and giving a more direct correlation to weight, are presented in Table 8.

The ICRP model predicts values for the absorbed dose, by multiplying the administered activity of each patient (A_0) by the corresponding dose coefficients available on ICRP Publication 80 (the ICRP Publication 80 is an addendum to ICRP Publication 53)[27], obtaining a dose value called D^{ICRP} in this work. This is called the ICRP method in this study, and will be considered the reference to which the other methods will be compared.

The other methods are:

(a) Method 1: This consists of multiplying the cumulated activity of each patient estimated by the ICRP model by the S-values of the most compatible voxel phantom estimated with MC simulations. This value is obtained using Equation 5, where $\tilde{A}_{kdn}$, $\tilde{A}_{lvr}$, $\tilde{A}_{spl}$, $\tilde{A}_{other}$ and $\tilde{A}_{bldrcnt}$ are the cumulated activities (MBq) in the kidney, liver, spleen, bladder contents and other (see ICRP for definition, which does not include liver, spleen, kidneys and bladder, as they would count twice), respectively, estimated by the ICRP 128 biokinetic model; and $S_{kdn<-kdn}$, $S_{kdn<-lvr}$, $S_{kdn<-spl}$, $S_{kdn<-other}$ and $S_{kdn<-bldrcnt}$ are the deposited energies (mGy/MBq) in the kidneys by simulating a source in the kidneys, liver, spleen, bladder contents and other, respectively. The dose estimation with this method was called D^1.

$$D^1(\text{mGy}) = \tilde{A}_{kdn} \times S_{kdn<-kdn} + \tilde{A}_{lvr} \times S_{kdn<-lvr} + \tilde{A}_{spl} \times S_{kdn<-spl} + \tilde{A}_{other} \times S_{kdn<-other} + \tilde{A}_{bldrcnt} \times S_{kdn<-bldrcnt} \quad (5)$$

(b) Method 2: In those cases where the phantoms with closest match to the patient by weight and by age were different, the alternative phantom to that chosen for method 1 was used for method 2. The dose estimation with this method was called D^2.

(c) Method 3: Equal to methods 1 and 2, but using the S-values obtained with the fitting exponential function as given by Equation 4. This gives S-values matching the exact weight of the patient. As no voxel phantoms used in this study weigh more than 30 kg the validity of this model is limited to this weight value. The value of dose obtained with this method was called D^3. The values are presented in Table 9.

Given that the *Child_21.7 kg* (the original CHILD phantom) and the *Child_21.5 kg* phantoms provide very similar S-values, resulting in deviations in absorbed dose estimation that is less than ~5%, the *Child_21.7 kg* phantom was not used altogether, and the *Child_21.5 kg* used instead, although the *Child_21.7 kg* was used for the calculations of the

Table 8. *S*-values obtained for each patient by fitting an exponential function to the values obtained with MC.

Patient	$S_{kidneys<-kidneys}$ (mGy/MBq)	$S_{kidneys<-liver}$ (mGy/MBq)	$S_{kidneys<-spleen}$ (mGy/MBq)	$S_{kidneys<other}$ (mGy/MBq)	$S_{kidneys<-bladdercontent}$ (mGy/MBq)
1	7.86×10^{-5}	7.26×10^{-7}	1.72×10^{-6}	3.36×10^{-6}	6.97×10^{-7}
2	4.92×10^{-5}	4.79×10^{-7}	1.29×10^{-6}	2.40×10^{-6}	3.46×10^{-7}
3	5.28×10^{-5}	5.11×10^{-7}	1.35×10^{-6}	2.53×10^{-6}	3.85×10^{-7}
4	4.58×10^{-5}	4.50×10^{-7}	1.23×10^{-6}	2.28×10^{-6}	3.12×10^{-7}
5	3.97×10^{-5}	3.97×10^{-7}	1.13×10^{-6}	2.06×10^{-6}	2.52×10^{-7}
6	4.92×10^{-5}	4.79×10^{-7}	1.29×10^{-6}	2.40×10^{-6}	3.46×10^{-7}
7	4.92×10^{-5}	4.79×10^{-7}	1.29×10^{-6}	2.40×10^{-6}	3.46×10^{-7}
8	4.58×10^{-5}	4.50×10^{-7}	1.23×10^{-6}	2.28×10^{-6}	3.12×10^{-7}
9	3.83×10^{-5}	3.84×10^{-7}	1.10×10^{-6}	2.01×10^{-6}	2.39×10^{-7}
10	4.27×10^{-5}	4.23×10^{-7}	1.18×10^{-6}	2.17×10^{-6}	2.80×10^{-7}
11	2.87×10^{-5}	2.97×10^{-7}	9.22×10^{-7}	1.63×10^{-6}	1.55×10^{-7}
12	3.45×10^{-5}	3.50×10^{-7}	1.03×10^{-6}	1.86×10^{-6}	2.04×10^{-7}
13	5.84×10^{-6}	7.24×10^{-8}	3.44×10^{-7}	5.20×10^{-7}	1.44×10^{-8}
14	4.56×10^{-6}	5.81×10^{-8}	2.95×10^{-7}	4.35×10^{-7}	9.94×10^{-9}
15	2.87×10^{-6}	3.86×10^{-8}	2.27×10^{-7}	3.12×10^{-7}	4.99×10^{-9}
16	3.97×10^{-7}	6.61×10^{-9}	6.46×10^{-8}	7.49×10^{-8}	2.57×10^{-10}
17	1.23×10^{-6}	1.81×10^{-8}	1.31×10^{-7}	1.69×10^{-7}	1.40×10^{-9}

Downloaded from http://rpd.oxfordjournals.org/ at City University, London on April 23, 2016

Table 9. Absorbed dose in the kidneys (mGy) calculated using the four different methods (D^{ICRP}, D^1, D^2 and D^3) for the 17 patients, divided into the five groups.

	Absorbed dose in the kidneys (mGy)													
Patient	Patient's weight	Patient's age	Closest match to ICRP	ICRP age correspondence of closest match phantom	Alternative phantom	[D^{ICRP}] (method A)	[D^1] (method B)	[D^2] Alternative phantom (method C)	[D^3] Using fitted *S*-factors to patient's weight	(D^1–D^{ICRP})/D^{ICRP} (%)	(D^2–D^{ICRP})/D^{ICRP} (%)	(D^3–D^{ICRP})/D^{ICRP} (%)	Weight deviation between alternative phantom and ref phantom (%)	Weight deviation between patient's weight and ref phantom (%)
1	3.4	2 months	Baby_9.5 kg	1 y	Baby_4.3 kg	19.12	17.63	37.80	28.22	−7.8	97.6	47.6	−54.7	−64.21
2	10.0	8 months	Baby_9.5 kg	1 y	—	29.53	27.22	—	27.54	−7.8	—	−6.8	—	5.3
3	9.0	10 months			—	28.12	25.93	—	28.12	−7.8	—	0.0	—	−5.3
4	11.0	10 months			Child_13.2 kg	28.12	25.93	17.16	24.48	−7.8	−39.0	−13.0	39.0	15.8
5	13.0	12 months			Child_13.2 kg	36.56	33.70	22.31	27.70	−7.8	−39.0	−24.2	39.0	36.8
6	10.0	13 months			—	30.37	28.00	—	28.33	−7.8	—	−6.7	—	5.3
7	10.0	16 months			—	32.62	30.07	—	30.43	−7.8	—	−6.7	—	5.3
8	11.0	17 months			Child_13.2 kg	31.78	29.30	19.39	27.66	−7.8	−39.0	−12.9	39.0	15.8
9	13.5	2 y			—	31.78	29.30	—	23.26	−7.8	—	−26.8	—	42.1
10	12.0	2 y			Child_13.2 kg	29.24	26.97	17.85	23.75	−7.8	−39.0	−18.8	39.0	26.3
11	17.6	3 y	Child_13.2 kg	5 y	Child_21.5 kg	24.98	26.94	17.23	27.65	7.9	−31.0	10.7	62.9	33.3
12	15.0	4 y			Child_21.5 kg	19.09	20.59	13.17	24.55	7.9	−31.0	26.5	62.9	13.6
13	40.0	11 y	Child_21.5 kg	10 y	Child_30 kg	21.09	20.85	15.53	6.32	−1.1	−26.4	−70.0	39.6	86.05
14	43.5	11 y			Child_30 kg	23.20	22.93	17.08	5.48	−1.1	−26.4	−76.4	39.6	102.3
15	50.0	15 y	Child_30 kg	15 y	—	18.72	18.80	—	3.88	0.4	—	−79.3	—	66.7
16	78.0	15 y			—	28.49	28.61	—	0.91	0.4	—	−96.8	—	160.0
17	62.0	16 y			—	20.35	20.44	—	1.88	0.4	—	−90.8	—	106.7

Downloaded from http://rpd.oxfordjournals.org/ at City University, London on April 23, 2016

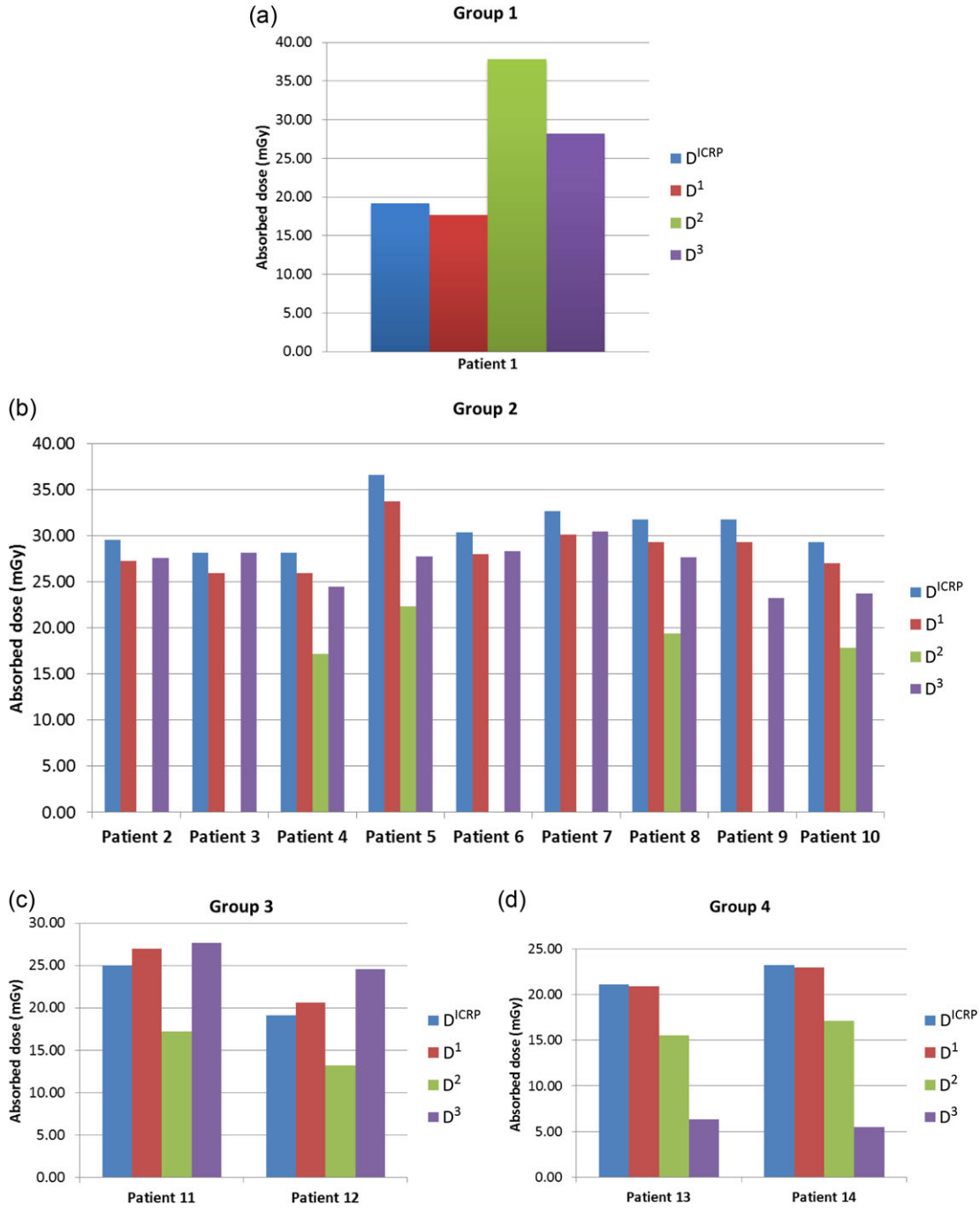

Figure 5. (**a**) Absorbed dose in the kidneys calculated by different methods (D^{ICRP}, D^1, D^2 and D^3) for Group 1. (**b**) Absorbed dose in the kidneys calculated by different methods (D^{ICRP}, D^1, D^2 and D^3) for Group 2. (**c**) Absorbed dose in the kidneys calculated by different methods (D^{ICRP}, D^1, D^2 and D^3) for Group 3. (**d**) Absorbed dose in the kidneys calculated by different methods (D^{ICRP}, D^1, D^2 and D^3) for Group 4. (**e**) Absorbed dose in the kidneys calculated by different methods (D^{ICRP}, D^1 and D^3) for Group 5.

Downloaded from http://rpd.oxfordjournals.org/ at City University, London on April 23, 2016

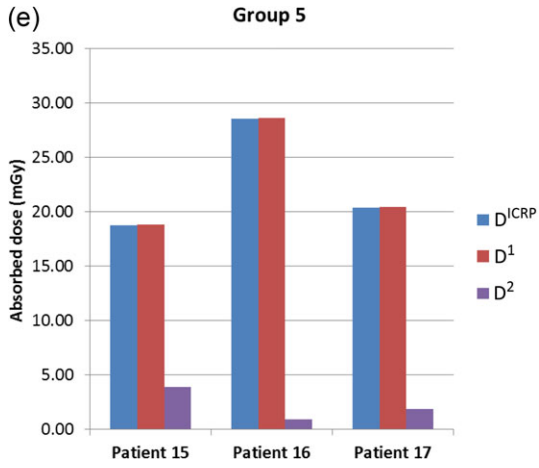

Figure 5. *Continued*

fitting exponential. The obtained results can be summarised as follows:

(a) For Group 1 (patient 1), as shown in Figure 5a, the method to which deviations to the ICRP values are minimal (−7.8%) is method D^1, using *Baby_9.5 kg*. Method D^2 would have used the *Baby_4.3 kg*, which leads to an absorbed dose value that deviates from the ICRP by ~97%. The difference in mass is very significant. Given that this patient's mass is 3.4 kg, this would in fact mean that realistically, in terms of weight, the *Baby_4.3 kg* phantom is more suited for dose calculations, as is shown by the use of method D^3, which fits the *S*-values to the real weight of the patient and estimates a dose much closer to that of method D^2. This in turn means that if one used the ICRP method the dose would have been underestimated by a factor of 50%. Finally it should be noted, again, that ICRP does not provide dose conversion coefficient data for newborns.

(b) For Group 2 (patients 2–10), as shown in Figure 5b, the mean value obtained for D^{ICRP}, D^1, D^2 and D^3 was 30.90(±2.67) mGy, 28.49 (±2.46) mGy, 19.18(±2.29) mGy and 26.81 (±2.41) mGy, respectively. The deviation between the kidney doses obtained with D^1 and D^{ICRP} is constant at −7.8%. In this case both the ICRP phantom and the Baby_9.5 kg are very similar to the patient's weight, which explains the small deviation in the values. In any case where there could be an alternative phantom used, the values obtained (D^2) are always smaller than those obtained using the closest match phantom. For method 3, D^3 values are always close to the ICRP values, although they decrease significantly when the weight of the patients is higher.

(c) For Group 3 (patients 11 and 12), as shown in Figure 5c, the values obtained for D^{ICRP} were 24.98 mGy and 19.09 mGy respectively, whereas for D^1 the values were 26.94 mGy and 20.59 mGy, using the phantom *Child_13.2 kg*'s obtained *S*-values. Considering that both patients' body mass is closer to that of phantom *Child_21.5 kg*, methods 2 and 3, using weight only as a parameter, would be more appropriate. However, the dose values D^2 are smaller whereas the dose values D^3 are bigger than the ICRP value.

(d) For Group 4 (patients 13 and 14), as shown in Figure 5d, the values obtained for D^{ICRP} were 21.09 mGy and 23.20 mGy respectively, whereas for D^1 the values were 20.85 mGy and 22.93 mGy, using the phantom *Child_21.5 kg*'s obtained *S*-values. Considering that both patients' body mass is closer to that of phantom *Child_30 kg*, methods 2 and 3, using weight only as a parameter, would be more appropriate. In this case both the values D^2 and D^3 are significantly smaller than the ICRP value. The values for D^3 deviate quite significantly (are ~70% smaller) from the ICRP ones. This is indicative that the phenomenological equation is inadequate to estimate doses for patients with a total body weight higher than 30 kg.

(e) For Group 5 (patients 15–17), as shown in Figure 5e, the mean value obtained for D^{ICRP}, D^1 and D^3 was 22.52(±5.23) mGy, 22.62(±5.25) mGy and 2.22(±1.51) mGy, respectively. The deviation between the kidney doses obtained with D^1 and D^{ICRP} is very small. However, unlike in Group 2, the ICRP phantom and the *Child_30 kg* are very different from the actual patient's weight, which explains the huge disparity found between the values of D^{ICRP} and D^1 with the values of D^3. This is again due to the fact that the phenomenological equation is inadequate to estimate doses for patients with a total body weight higher than 30 kg.

Estimation of dose coefficients to the kidney

The dose coefficients are established for the organs involved in the biodistribution of radiopharmaceuticals, and are based on the MIRD system[28]. These coefficients represent absorbed dose per unit of administered activity (mGy/MBq), and are used clinically for absorbed dose estimation to the organs, in this case, to the kidney. Based on the different methods used to estimate absorbed doses besides the ICRP 80 in this study, new dose coefficients have been computed for the kidneys and compared with those from the ICRP model, as shown in Table 10.

Figure 6 shows the dose coefficients variation with the different methodologies.

Downloaded from http://rpd.oxfordjournals.org/ at City University, London on April 23, 2016

Table 10. Dose conversion factors for the kidneys.

(Group)	ICRP age match	Method 1	Method 2	Method 3	ICRP 80
Patients 1–10	1 y	$7.0 \times 10^{-1} \pm 4.3 \times 10^{-5}$	$7.2 \times 10^{-1} \pm 5.1 \times 10^{-1}$	$7.1 \times 10^{-1} \pm 6.8 \times 10^{-2}$	7.6×10^{-1}
Patients 11–12	5 y	$4.6 \times 10^{-1} \pm 1.7 \times 10^{-5}$	$3.0 \times 10^{-1} \pm 9.2 \times 10^{-6}$	$5.1 \times 10^{-1} \pm 5.4 \times 10^{-2}$	4.3×10^{-1}
Patients 13–14	10 y	$3.0 \times 10^{-1} \pm 4.6 \times 10^{-5}$	$2.2 \times 10^{-1} \pm 2.7 \times 10^{-5}$	$8.0 \times 10^{-2} \pm 1.4 \times 10^{-2}$	3.0×10^{-1}
Patients 15–17	15 y	$2.2 \times 10^{-1} \pm 3.2 \times 10^{-5}$	—	$1.4 \times 10^{-2} \pm 9.4 \times 10^{-3}$	2.2×10^{-1}

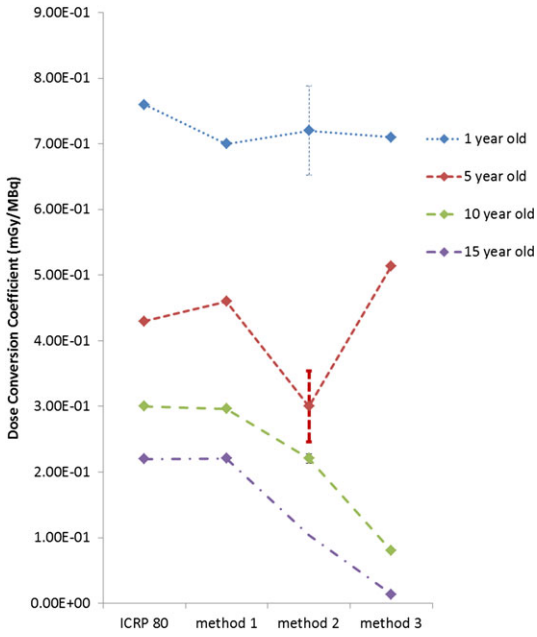

Figure 6. Dose conversion coefficients (mGy/MBq) for the four different methodologies. The error bars correspond to standard deviations. For the value for the dose coefficient for 1 year old, method 1, the error bar is not drawn.

The four different methods do not yield significant variations, with the notable exception of method 3, which gives dose conversion coefficient values that are much smaller for the groups of patients 13–14 and 15–17. This method is inadequate to estimate dose in this case, as no voxel phantom used in this study has a body weight higher than 30 kg, and all the aforementioned patients have a total body weight far exceeding this value.

CONCLUSIONS

Absorbed dose in the kidneys of 17 paediatric patients undergoing renal scintigraphies was estimated by means of biokinetic models, and dose coefficients from reference ICRP data (method ICRP). The absorbed dose was also assessed by calculating the individual *S*-values in the kidneys using MC simulations, using two possible alternative voxel phantoms (methods 1 and 2) and finally by fitting the previously MC obtained *S*-values as a function of the patients' body weight to a phenomenological function used for the purpose (method 3). This allowed for the estimation of dose coefficients using four different methodologies and to a comparison of these values.

MC simulations can be used to compute the dose coefficients, and provide a complementary methodology to be compared with the established ICRP models. By scaling the two available voxel phantoms with specific ages (2 months and 7 y) to match the ICRP values for kidney mass and height for 1 year, 5 year, 10 year and 15 year olds, by changing voxel volumes, a valid comparison to the ICRP values is possible.

As the dose to the kidney in the case of renal scintigraphies using 99m-TC-DMSA is mostly due to self-irradiation (where the beta particles play an important part) as well as irradiation from the rest of the body (the liver and the spleen account for a very low percentage of the total dose to the kidney), the kidney mass of the used phantoms will play a strong role in the dose assessment. This is visible in the different results, obtained for each group, as the kidney size and mass change in the phantoms used for the calculations, suggesting that a more convenient parameter for providing ICRP values is mass, rather than age. ICRP seems to have followed a similar approach used in pharmacokinetics to determine the correct dosage to paediatric patients from drugs, by age, although this seems to be an open issue, as the weight–age variation is not linear[29]. Also, the given values in the models tend to be the average for a 'typical' child or baby with a specific age, when in clinical practice there can be huge disparities between the patient's characteristics and those of the models (as can be noticed in this study).

Because of this, the dose coefficients established by ICRP can be either underestimating the absorbed dose (such as in the case of patient 1, where the body weight is closer to the value provided to a newborn), or overestimating it, such as in the case of patients 13–17, where the body mass of the patients far exceeds the body weight of the voxel phantoms, although it is close to the ICRP data provided for 10 and 15 years olds. In fact the voxel phantoms used

Downloaded from http://rpd.oxfordjournals.org/ at City University, London on April 23, 2016

in this study do not have the same body weight as the ICRP phantoms, for any age, and the weight difference between the total body weight of the used voxel phantoms and the ICRP values increases with age, being higher for 10 and 15 years old.

Since it is contra-indicated to expect a clinical implementation of CT scans to construct individual voxel phantoms of each patient, the most accurate methodology would perhaps be to build a variety of phantoms at different ages and adjust them only within a much smaller weight and height variety. With this, one could construct *S*-value curves for different anatomical parameters (age, height and girth). Clinicians and medical physicists could estimate a more accurate value of dose by correlating one of these phantoms with their patient. Perhaps they can even test two different values (if the values for the patients are closer in mass to one but in height to the other and vice-versa) and obtain two different values of dose, which could give them an idea of the uncertainty of their estimation. This could clearly lead to dose optimisation, which is a fundamental pillar of radiation protection. This is especially valid for paediatric patients as they are known to be more radiosensitive than adults. It is not unfair to assume that such methods are within practical reach of clinicians/medical physicists, or other workers.

ACKNOWLEDGEMENTS

The authors would like to thank the staff in the Nuclear Medicine department of Hospital Garcia de Orta for their support in making the measurements for this study and to J. Bento for valuable discussions. Finally V. de Sousa would like to thank the University of Coimbra.

REFERENCES

1. Teles, P., de Sousa, M. C., Paulo, G., Santos, G., Pascoal, A., Cardoso, G., Lança, I., Matela, N., Janeiro, L., Sousa, P., Carvoeiras, P., Parafita, R., Santos, A. I., Simãozinho, P. and Vaz, P. *Estimation of the collective dose in the Portuguese population due to medical procedures in 2010*. Radiat. Prot. Dosimetry **154**, 446–458 (2013).
2. Frush, D. P. and Applegate, K. E. *Radiation risk from medical imaging in children*. In: Evidence-based Imaging in Pediatrics – Optimizing imaging in Pediatric Patient Care. Medina, L. S., Applegate, K. E. and Blackmore, C. C., Eds. (New York: Springer) pp. 25–39 (2010).
3. National Council on Radiation Protection and Measurement. *Ionizing Radiation Exposure of the Population of the United States*. NCRP Report No. 160 (2009).
4. Fahey, F. H., Treves, S. T. and Adelstein, S. J. *Minimizing and communicating radiation risk in Pediatric Nuclear Medicine*. J. Nucl. Med. Technol. **40**, 13–24 (2012).
5. United Nations Scientific Committee on the Effects of Atomic Radiation UNSCEAR 2013 Report – Volume II: Scientific Annex B – Effects of radiation exposure of children. II (2013).
6. National Research Council, Committee to Assess Health Risks from Exposure to Low Levels of Ionizing Radiation. *Health Risks from Exposure to Low Levels of Ionizing Radiation: BEIR VII Phase 2* (2006).
7. Loevinger, R. and Berman, M.-A. *A schema for absorbed-dose calculations for biologically distributed radionuclides*. J. Nucl. Med. **9**, 7–14 (1968).
8. International Committee on Radiological Protection Publication 53. *Radiation Dose to Patients from Radiopharmaceuticals*. Ann. ICRP **18** (1988).
9. International Committee on Radiological Protection Publication 128. *Radiation Dose to Patients from Radiopharmaceuticals: A Compendium of Current Information Related to Frequently used Substances*. Ann. ICRP **25** (2015).
10. Bolch, W. E., Eckerman, K. F., Sgouros, G. and Thomas, S. R. *MIRD Pamphlet No. 21: A generalized schema for radiopharmaceutical dosimetry—standardization of nomenclature*. J. Nucl. Med. **50**, 477–484, (2009).
11. Eberlein, U., Bröer, J. H., Vandevoorde, C., Santos, P., Bardiès, M. Bacher, K., Nosske, D. and Lassmann, M. *Biokinetics and dosimetry of commonly used radiopharmaceuticals in diagnostic nuclear medicine – a review*. Eur. J. Nucl. Med. Mol. Imaging. **38**, 2269–2281 (2011).
12. Leggett, R. W., Eckerman, K. F. and Meck, R. A. *Reliability of current biokinetic and dosimetric models for radionuclides: a pilot study*. OAK RIDGE Nat. Lab. (2008). doi:10.2172/939651.
13. Zankl, M., Petoussi-Henss, N., Fill, U. and Regulla, D. *The application of voxel phantoms to the internal dosimetry of radionuclides*. Radiat. Prot. Dosimetry **105**, 539–547 (2003).
14. Hadid, L., Gardumi, A. and Desbrée, A. *Evaluation of absorbed and effective doses to patients from radiopharmaceuticals using the ICRP 110 computational phantoms and ICRP 103*. Radiat. Prot. Dosimetry **156**, 141–159 (2013).
15. Hadid, L., Desbrée, A., Schlattl, H., Franck, D., Blanchardon, E. and Zankl, M. *Application of the ICRP/ICRU ICRP computational phantoms to internal dosimetry: calculation of specific absorbed fractions of energy for photons and electrons*. Phys. Med. Biol. **55**, 3631–3641 (2010).
16. Parach, A. A., Rajabi, H. and Askari, M. A. *Assessment of MIRD data for internal dosimetry using the GATE Monte Carlo code*. Radiat. Environ. Biophys. **50**, 441–450 (2011).
17. Evans, K., Lythgoe, M. F., Anderson, P. J., Smith, T. and Gordon, I. *Biokinetic behavior of Technetium-99m-DMSA in children*. J. Nucl. Med. **37**, 1331–1335 (1996).
18. Smith, T., Evans, K., Lythgoe, M. F., Anderson, P. J. and Gordon, I. *Radiation dosimetry of Technetium-99m-DMSA in children*. J. Nucl. Med. **37**, 1336–1342 (1996).
19. International Committee on Radiological Protection Addendum 3 to ICRP Publication 53. *Radiation Dose to Patients from Radiopharmaceuticals*. ICRP Publication 106. Ann. ICRP **38**, (2008).
20. *MCNPX User's Manual, Version 2.7.0* (Los Alamos, NM: Los Alamos National Laboratory) (2011).

Downloaded from http://rpd.oxfordjournals.org/ at City University, London on April 23, 2016

21. Zankl, M., Veit, R., Williams, G., Schneider, K., Fendel, H., Petoussi, N. and Drexler, G. *The construction of computer tomographic phantoms and their application in radiology and radiation protection*. Radiat. Env. Biophys. **27**, 153–164 (1988).
22. Cristy, M. and Eckerman, K. F. *Specific absorbed fractions of energy at various ages from internal photon sources*. Oak Ridge National Laboratory report. Health and Safety Division ORNL/TM-8381 (1987).
23. International Committee on Radiological Protection Publication 89. *Basic Anatomical and Physiological Data for use in Radiological Protection ICRP Values*. Ann. ICRP **32** (2002).
24. Table of radioactive isotopes. Available on http://nucleardata.nuclear.lu.se/toi/nuclide.asp?iZA=430399. (Accessed on 8 March 2016).
25. Lamart, S., Bouville, A., Simon, S. L., Eckerman, K. F., Melo, D. and Lee, C. *Comparison of internal dosimetry factors for three classes of adult computational phantoms with emphasis on I-131 in the thyroid*. Phys. Med. Biol. **56**, 7317–7335 (2012).
26. Lassmann, M. and Treves, S. T. *Paediatric radiopharmaceutical administration: harmonization of the 2007 EANM paediatric dosage card (version 1.5.2008) and the 2010 North American consensus guidelines*. Eur. J. Nucl. Med. Mol. Imaging. **41**, 1036–1041 (2014).
27. International Committee on Radiological Protection Addendum to ICRP Publication 53. *Radiation Dose to Patients from Radiopharmaceuticals*. ICRP Publ. 80. Ann. ICRP **28** (1998).
28. Snyder, W. S., Ford, M. R. and Warner, G. G. *MIRD Pamphlet No. 5: Estimates of absorbed fractions for nonenergetic photon sources uniformly distributed in various organs of a heterogeneous phantom*. J. Nucl. Med. **5**(Suppl. 3) (1978).
29. Cella, M., Knibbe, C., Danhof, M., Della Pasqua, O. *What is the right dose for children?* Br. J. Clin. Pharmacol. **70**(4), 597–603 (2010).

Downloaded from http://rpd.oxfordjournals.org/ at City University, London on April 23, 2016